Journal of Statistical Physics, Vol. 80, Nos. 1/2, 1995

Asymmetric Exclusion Model with Two Species: Spontaneous Symmetry Breaking

M. R. Evans,[1] D. P. Foster,[2] C. Godrèche,[2,3] and D. Mukamel[3,4]

Received August 10, 1994; final December 30, 1994

A simple two-species asymmetric exclusion model is introduced. It consists of two types of oppositely charged particles driven by an electric field and hopping on an open chain. The phase diagram of the model is calculated in the mean-field approximation and by Monte Carlo simulations. Exact solutions are given for special values of the parameters defining its dynamics. The model is found to exhibit two phases in which spontaneous symmetry breaking takes place, where the two currents of the two species are not equal.

KEY WORDS: Stochastic lattice gas; excluded volume; steady states; phase transitions; spontaneous symmetry breaking.

1. INTRODUCTION

One-dimensional models of particles hopping in a preferred direction provide simple nontrivial realizations of system out of thermal equilibrium.[1-3] For example, a system of particles with hard-core interactions, which make nearest-neighbor hops in a preferred direction on a one-dimensional lattice, may be mapped onto a discretized growth model in $1+1$ dimensions.[4-8] Such a system of particles is known as an asymmetric exclusion model.[9] This class of models and their generalizations in two dimensions have been studied as examples of driven diffusive systems.[10,11] They exhibit interesting collective phenomena, such as boundary-induced phase transitions[12]

[1] Laboratoire de Physique Statistique (Laboratoire associé au Centre National de la Recherche Scientifique et aux Universités Paris VI et Paris VII), École Normale Supérieure, 75231, Paris Cedex 05, France.

[2] Service de Physique de l'État Condensé, Centre d'Études de Saclay, 91191 Gif-sur-Yvette Cedex, France.

[3] Newton Institute for Mathematical Sciences, Cambridge CB2 OEH, United Kingdom.

[4] Department of Physics of Complex Systems, Weizmann Institute of Science, Rehovot, Israel.

0022-4715/95/0700-0069$07.50/0

and phase transitions induced by a single defect in the lattice.[8, 13] Also, the dynamics of shocks or moving fronts may be studied within these models.[14–18]

The totally asymmetric exclusion model corresponds to the case where particles are restricted to move only forward. This model has been solved exactly in one dimension and with open boundary conditions.[19–21] A simple way of obtaining the solution is to represent the steady state of the system by a product of noncommuting matrices.[20] This method has been extended to the case of a system consisting of two species of particles moving on a ring.[22] This allows the structure of shocks to be examined.

In the present work we study a totally asymmetric one-dimensional exclusion model consisting of two species of particles with open boundary conditions. The two species of particles move in opposite directions and for convenience we refer to them as "positive" and "negative" particles. This model possesses a rich phase diagram and is found to exhibit *spontaneous symmetry breaking*, which is an unusual phenomenon in one dimension. A preliminary discussion of this model has been given in ref. 23.

There are several physical situations modeled by exclusion processes for which two species of particles are required. Repton models of diffusion of polymer chains and gel electrophoresis may be considered as exclusion processes with two species of particles,[24–27] as can certain models of growing interfaces in $1+1$ dimensions.[8, 13]

Let us define the model we consider. Each site of a one-dimensional lattice of length N may be occupied by a positive particle or a negative particle or be empty. The system evolves according to a stochastic dynamical rule as follows. In each infinitesimal time step dt the following events may occur at each nearest-neighbor pair of sites i, $i+1$ $(1 \leqslant i \leqslant N-1)$:

$$\begin{aligned} (+)_i(0)_{i+1} &\to (0)_i(+)_{i+1} \quad \text{with probability } dt \\ (+)_i(-)_{i+1} &\to (-)_i(+)_{i+1} \quad \text{with probability } q\,dt \\ (0)_i(-)_{i+1} &\to (-)_i(0)_{i+1} \quad \text{with probability } dt \end{aligned} \tag{1.1}$$

where $(+)_i$ and $(-)_i$ indicate a positive or negative particle at site i, respectively, and $(0)_i$ indicates that site i is empty.

At the boundaries, particles may be introduced and removed. Thus in each infinitesimal time step dt, the following events may occur at the left-hand boundary $(i=1)$:

$$\begin{aligned} (0)_1 &\to (+)_1 \quad \text{with probability } \alpha\,dt \\ (-)_1 &\to (0)_1 \quad \text{with probability } \beta\,dt \end{aligned} \tag{1.2}$$

and the following at the right-hand boundary ($i = N$):

$$\begin{aligned} (0)_N &\to (-)_N \qquad \text{with probability} \quad \alpha\, dt \\ (+)_N &\to (0)_N \qquad \text{with probability} \quad \beta\, dt \end{aligned} \tag{1.3}$$

This model may be thought of in terms of two single-species totally asymmetric exclusion processes. The processes interact through the exclusion interaction and through the exchange of + and − particles at rate q. The phase diagram for the single-species model, obtained by a matrix method,[20] consists of a maximal-current phase, a high-density phase, and a low-density phase. For certain cases ($\beta = 1$ or $\alpha = \infty$) we have been able to use a similar method to solve our model exactly and we find phases analogous to the maximal-current and low-density phases of the single-species model. These are examples of what we shall refer to as symmetric phases, for which the charge currents of positive and negative particles are equal: $J^+ = J^-$. In this work we show the existence of phases where $J^+ \neq J^-$. In theses phases the symmetry of the dynamics (1.1)–(1.3) under interchange of positive and negative particles and of their directions is spontaneously broken.

For the sake of clarity let us summarize our main results:

(i) Through an exact solution given by the matrix method for $\beta = 1$ we show that the two-species exclusion process exhibits a boundary-induced phase transition, between a low-density phase and a power-law phase, similar to that of the one-species model. This transition only occurs for $q < 2$.

(ii) By use of mean-field theory we explore other ranges of β. For $q = 1$ the mean-field equations can be solved analytically and we demonstrate the existence of two broken symmetry phases and calculate the mean-field phase diagram. These broken symmetry phases provide a novel class of boundary-induced phase transitions.

For $q < 1$ we show by comparison of the exact solution and mean-field theory that the latter incorrectly predicts the order of the transition. This is surprising since for the one-species exclusion process the mean-field predictions for the phase diagram are correct.[19] On the other hand, for $q = 1$ the predictions of the mean-field theory (in particular those pertaining to the broken symmetry phases) are well borne out by Monte Carlo simulations.

The paper is organized as follows. In Section 2 we present the exact solutions for the cases $\beta = 1$ and $\alpha = \infty$—technical details being left to Appendices A and B—and discuss the resulting phase diagram and density

profiles. In Section 3 we investigate the mean-field approximation to the stochastic model, first solving the case $q=1$ then studying $q \neq 1$ numerically. In Section 4 we show that Monte Carlo simulations provide strong evidence that the broken symmetry phases exist in the stochastic model. We conclude in Section 5 and discuss our results in terms of an interface model.

2. MATRIX SOLUTIONS

In this section we deal with two cases where an exact solution for the stationary state of the model can be obtained using the matrix method introduced in ref. 20. This method has previously been applied to study the present model in a ring geometry.[22]

Before reviewing this approach we define some notation. We introduce two occupation numbers, τ_i and θ_i, for each site i, where $\tau_i = 1$ if site i is occupied by a positive particle and 0 otherwise. Similarly, $\theta_i = 1$ if site i is occupied by a negative particle and 0 otherwise. As the particles are subjected to an excluded-volume interaction, only one of τ_i and θ_i may be nonzero and the configuration of the system is uniquely defined by the set of occupation numbers $\{\tau_i, \theta_i\}$. Here we are interested in the nonequilibrium steady state ($t \to \infty$) of the system, that is, $P_N(\{\tau_i, \theta_i\})$ (the probability of finding the system of size N in configuration $\{\tau_i, \theta_i\}$).

It is convenient to consider unnormalized weights $f_N(\{\tau_i, \theta_i\})$ defined through

$$P_N(\{\tau_i, \theta_i\}) = \frac{f_N(\{\tau_i, \theta_i\})}{Z_N} \tag{2.1}$$

with

$$Z_N = \sum_{\{\tau_i, \theta_i\}} f_N(\{\tau_i, \theta_i\}) \tag{2.2}$$

Following ref. 20, we make the ansatz that $f_N(\{\tau_i, \theta_i\})$ may be constructed as

$$f_N(\{\tau_i, \theta_i\}) = \langle W | \prod_{i=1}^{N} [\tau_i \mathbf{D} + \theta_i \mathbf{E} + (1 - \tau_i - \theta_i) \mathbf{A}] | V \rangle \tag{2.3}$$

The expression in the brackets implies the presence of a matrix $\mathbf{D}$ if site i is occupied by a positive particle, a matrix $\mathbf{E}$ if site i is occupied by a negative particle, and a matrix $\mathbf{A}$ if site i is empty. The action of the vectors $|V\rangle$ and $\langle W|$ on the matrix product gives a scalar for f_N. Formally the

solution of the problem reduces to finding a set of matrices and vectors such that f_N is a stationary solution of the master equation describing the time evolution of the system.

By using this ansatz we found an exact solution in the following two cases.

2.1. Solution for $\alpha = \infty$

When $\alpha \to \infty$ it is clear from (1.2), (1.3) that, as soon as a hole appears at a boundary site, it is removed. Thus in the steady state the system will be devoid of holes. This is equivalent to saying that any time a matrix **A** occurs in the system the corresponding weight is zero. The dynamics given in Eqs. (1.1)–(1.3) reduces to

$$\begin{aligned} (+)_i(-)_{i+1} &\to (-)_i(+)_{i+1} \qquad \text{with probability } q\,dt \\ (-)_1 &\to (+)_1 \qquad \text{with probability } \beta\,dt \\ (+)_N &\to (-)_N \qquad \text{with probability } \beta\,dt \end{aligned} \tag{2.4}$$

If one now calls the negative particles "holes," the problem reduces to the single-species asymmetric exclusion process with open boundaries, here with the hop rate in the bulk set to q. Rescaling time so that this hop rate is unity, we find that the model reduces to a one-species dynamics with effective rates of adding and removing a particle equal to β/q.

For this model the matrices **D**, **E** may be chosen to satisfy

$$\langle W|\,\mathbf{E} = \frac{q}{\beta}\langle W|; \qquad \mathbf{D}\,|V\rangle = \frac{q}{\beta}\,|V\rangle; \qquad \mathbf{DE} = \mathbf{D} + \mathbf{E} \tag{2.5}$$

Explicit forms for the matrices and vectors satisfying these conditions are given in ref. 20, and using results given in this reference, one finds in the limit $N \to \infty$ two possible phases:

For $\beta/q > 1/2$. The current is given by $J^+ = q/4$ and the density of positive particles decays as one moves away from the left-hand boundary to a constant bulk value according to a power law

$$\langle \tau_n \rangle \simeq \frac{1}{2} + \frac{1}{2\sqrt{\pi}\, n^{1/2}} + \cdots \qquad \text{for large } n \tag{2.6}$$

One can deduce the decay in the density of negative particles and the decays at the right-hand boundary through the symmetry $\langle \tau_i \rangle = \langle \theta_{N-i+1} \rangle$ and $\langle \tau_i \rangle + \langle \theta_i \rangle = 1$.

For $\beta/q < 1/2$. The current is given by $J^+ = \beta/q(1-\beta/q)$ and the density profile is linear in the bulk

$$\langle \tau_{Nx} \rangle \simeq \frac{\beta}{q} + x\left(1 - 2\frac{\beta}{q}\right) \tag{2.7}$$

This phase can be understood as a superposition of shocks, the position of which may be anywhere on the lattice with equal probability, giving rise to the linear density profile.[19]

2.2. Solution for $\beta = 1$

By considering the master equation for the time evolution of the system and the form of f_N in (2.3), it is shown in Appendix A that the matrices and vectors satisfy the following algebra. From the left-hand boundary

$$\langle W| \mathbf{E} = q\langle W| \tag{2.8}$$

$$\langle W| \mathbf{A} = \frac{q}{\alpha}\langle W| \tag{2.9}$$

from the right-hand boundary

$$\mathbf{D}\,|V\rangle = q\,|V\rangle \tag{2.10}$$

$$\mathbf{A}\,|V\rangle = \frac{q}{\alpha}\,|V\rangle \tag{2.11}$$

and from the bulk

$$\mathbf{DA} = q\mathbf{A} \tag{2.12}$$

$$\mathbf{AE} = q\mathbf{A} \tag{2.13}$$

$$\mathbf{DE} = \mathbf{D} + \mathbf{E} \tag{2.14}$$

Equation (2.14) implies that **D** and **E** either commute or are of infinite dimension.[20] In the commuting case one may as well take scalars since only the action of **D**, **E** on the boundary vectors matters. Then from (2.8), (2.10), and (2.14) one finds that $q = 2$. So, if $q \neq 2$, one must use infinite-dimensional matrices for **D** and **E**.

If one chooses

$$\langle W| V\rangle = 1 \tag{2.15}$$

then it may be seen from Eqs. (2.9) and (2.11)–(2.13) that a suitable choice for **A** is

$$\mathbf{A} = \frac{q}{\alpha} |V\rangle\langle W| \tag{2.16}$$

and we are left to satisfy (2.8), (2.10), and (2.14). The algebra given in Eqs. (2.8)–(2.14) is independent of the basis chosen, and while in principle one may perform the calculation without appeal to a basis, here we choose to work with the following representation:

$$\langle W| = \langle 1|; \qquad |V\rangle = |1\rangle \tag{2.17}$$

We have used the notation $\langle x| = \delta_{i,x}$ and $|x\rangle = \delta_{x,j}$; hence

$$\mathbf{A} = \frac{q}{\alpha} |1\rangle\langle 1| \tag{2.18}$$

and one can check that

$$\mathbf{D} = \begin{pmatrix} q & b & 0 & 0 & \cdots \\ 0 & 1 & 1 & 0 & \cdots \\ 0 & 0 & 1 & 1 & \cdots \\ 0 & 0 & 0 & 1 & \cdots \\ \vdots & \vdots & \vdots & \vdots & \end{pmatrix}, \qquad \mathbf{E} = \begin{pmatrix} q & 0 & 0 & 0 & \cdots \\ b & 1 & 0 & 0 & \cdots \\ 0 & 1 & 1 & 0 & \cdots \\ 0 & 0 & 1 & 1 & \cdots \\ \vdots & \vdots & \vdots & \vdots & \end{pmatrix} \tag{2.19}$$

satisfy (2.8)–(2.14), where

$$b^2 = q(2-q) \tag{2.20}$$

Current and Density Profiles for $\beta = 1$. It follows from (2.1) that the average density of positive particles at site i is given by

$$\langle \tau_i \rangle = \frac{1}{Z_N} \sum_{\{\tau_k, \theta_k\}} \tau_i f_N(\{\tau_k, \theta_k\}) \tag{2.21}$$

Writing down similar expressions for $\langle \theta_i \rangle$ and $\langle \sigma_i \rangle$, where $\sigma_i = 1 - \tau_i - \theta_i$ is the occupation number of holes at site i, and substituting in the explicit forms for f_N and Z_N, we find

$$\langle \tau_i \rangle = \frac{\langle W| \mathbf{G}^{i-1}\mathbf{D}\mathbf{G}^{N-i} |V\rangle}{\langle W| \mathbf{G}^N |V\rangle} \tag{2.22}$$

$$\langle \theta_i \rangle = \frac{\langle W| \mathbf{G}^{i-1}\mathbf{E}\mathbf{G}^{N-i} |V\rangle}{\langle W| \mathbf{G}^N |V\rangle} \tag{2.23}$$

$$\langle \sigma_i \rangle = \frac{\langle W| \mathbf{G}^{i-1}\mathbf{A}\mathbf{G}^{N-i} |V\rangle}{\langle W| \mathbf{G}^N |V\rangle} = \frac{q}{\alpha} \frac{\langle W| \mathbf{G}^{i-1} |V\rangle\langle W| \mathbf{G}^{N-i} |V\rangle}{\langle W| \mathbf{G}^N |V\rangle} \tag{2.24}$$

where

$$\mathbf{G} = \mathbf{D} + \mathbf{A} + \mathbf{E} \tag{2.25}$$

and we have used the expression for $\mathbf{A}$ given in Eq. (2.16).

Since a positive particle moves forward with rate one if there is a hole to its right and rate q if there is a negative particle to its right, the current J^+ of positive particles between sites i and $i+1$ is given by the following correlation function:

$$J^+ = \langle \tau_i(\sigma_{i+1} + q\theta_{i+1}) \rangle \tag{2.26}$$

Similarly the current of negative particles (with our convention that this current is positive from right to left) is given by

$$J^- = \langle (\sigma_i + q\tau_i)\, \theta_{i+1} \rangle \tag{2.27}$$

Using the matrix algebra given in Eqs. (2.8)–(2.14), we have

$$\begin{aligned} J^+ &= \frac{\langle W|\, \mathbf{G}^{i-1}\mathbf{D}(\mathbf{A}+q\mathbf{E})\, \mathbf{G}^{N-i-1}\, |V\rangle}{\langle W|\, \mathbf{G}^N\, |V\rangle} = q\, \frac{\langle W|\, \mathbf{G}^{N-1}\, |V\rangle}{\langle W|\, \mathbf{G}^N\, |V\rangle} \\ J^- &= \frac{\langle W|\, \mathbf{G}^{i-1}(\mathbf{A}+q\mathbf{D})\, \mathbf{E}\mathbf{G}^{N-i-1}\, |V\rangle}{\langle W|\, \mathbf{G}^N\, |V\rangle} = q\, \frac{\langle W|\, \mathbf{G}^{N-1}\, |V\rangle}{\langle W|\, \mathbf{G}^N\, |V\rangle} \end{aligned} \tag{2.28}$$

This expression for the current is independent of i, as it should be, since the system is in a stationary state, and is given directly in terms of the matrix elements of powers of $\mathbf{G}$. We shall start by looking at these matrix elements, hence calculating J and $\langle \sigma_i \rangle$, which will enable us to find and interpret the phase diagram for $\beta = 1$.

Recall that, from (2.18), (2.19), and (2.25) we may choose $\mathbf{G}$ as

$$\mathbf{G} = \begin{pmatrix} a & b & 0 & 0 & \cdots \\ b & 2 & 1 & 0 & \cdots \\ 0 & 1 & 2 & 1 & \cdots \\ 0 & 0 & 1 & 2 & \cdots \\ \vdots & \vdots & \vdots & \vdots & \end{pmatrix} \tag{2.29}$$

where

$$a = 2q + q/\alpha \qquad \text{and} \qquad b^2 = q(2-q) \tag{2.30}$$

In Appendix B we show that as $n \to \infty$, $\langle W|\, \mathbf{G}^n\, |V\rangle$ has the following asymptotic forms:

(i) For $q/\alpha < (q-2)^2$ and $q < 2$

$$\langle W| \mathbf{G}^n |V\rangle \simeq \frac{4^{n+1}}{\sqrt{\pi}\, n^{3/2}} \frac{q(2-q)}{[(q-2)^2 - q/\alpha]^2} \tag{2.31}$$

(ii) For $q/\alpha = (q-2)^2$ and $q < 2$

$$\langle W| \mathbf{G}^n |V\rangle \simeq \frac{4^n}{\sqrt{\pi}\, n^{1/2}} \frac{1}{q(2-q)} \tag{2.32}$$

(iii) For $q \geqslant 2$, or $q/\alpha > (q-2)^2$ and $q < 2$,

$$\langle W| \mathbf{G}^n |V\rangle \simeq \frac{(1-x^2)}{1-(1-q)^2 x^2} \left[\frac{(x+1)^2}{x}\right]^n \tag{2.33}$$

where

$$x = \frac{2(q-1) + q/\alpha - [4(q-1)\, q/\alpha + q^2/\alpha^2]^{1/2}}{2(q-1)^2} \tag{2.34}$$

One can check that for $q = 2$, (2.33) reduces to $\langle W| \mathbf{G}^n |V\rangle = (4 + 2/\alpha)^n$, as it should in this case since the 1, 1 element of $\mathbf{G}$ decouples from the rest of the matrix. Using these asymptotic forms and (2.28) to calculate the asymptotic forms of the current, we identify two phases:

(a) For $q < 2$ and $q/\alpha \leqslant (q-2)^2$

$$J = \frac{q}{4} \tag{2.35}$$

(b) For $q \geqslant 2$, or $q < 2$ and $q/\alpha > (q-2)^2$,

$$J = \frac{qx}{(x+1)^2} \tag{2.36}$$

We will refer to phase (a) as a power-law phase and to phase (b) as an exponential phase, the reason being that in the power-law phase, Eq. (2.24) implies that the density of holes decays to zero as a power law of the distance from the boundary

$$\langle \sigma_n \rangle \simeq \begin{cases} \dfrac{1}{\sqrt{\pi}\, n^{3/2}} \dfrac{q^2(2-q)}{\alpha[(q-2)^2 - q/\alpha]^2} & \text{for } q < 2, \dfrac{q}{\alpha} < (q-2)^2, \text{ and } n \text{ large} \\ \dfrac{1}{2\sqrt{\pi}\, n^{1/2}} \dfrac{1}{\alpha(2-q)} & \text{for } q < 2, \dfrac{q}{\alpha} = (q-2)^2, \text{ and } n \text{ large} \end{cases} \tag{2.37}$$

whereas on the exponential phase the density of holes decays exponentially to a bulk density given by

$$\langle \sigma_n \rangle \to \frac{q}{\alpha} \frac{(1-x^2)}{1-(1-q)^2 x^2} \frac{x}{(x+1)^2} \tag{2.38}$$

for $q \geqslant 2$, or $q < 2$, $q/\alpha > (q-2)^2$, and n large.

One should note from (2.35), (2.36) that in the power-law phase the current is maximal, i.e., greater than in the exponential phase.

In order to calculate the particle densities one can consider

$$\langle \tau_i \rangle = \sum_{p=2}^{i} d_p + \langle \tau_1 \rangle \tag{2.39}$$

where

$$d_p = \langle \tau_p \rangle - \langle \tau_{p-1} \rangle = \frac{\langle W | \mathbf{G}^{p-2} [\mathbf{GD} - \mathbf{DG}] \mathbf{G}^{N-p} | V \rangle}{\langle W | \mathbf{G}^N | V \rangle} \tag{2.40}$$

Now from (2.19) one can check that

$$\begin{aligned} \mathbf{GD} - \mathbf{DG} = & -b^2 |1\rangle\langle 1| + b(a-q-1) |1\rangle\langle 2| \\ & + b(q-1) |2\rangle\langle 1| + (b^2-1) |2\rangle\langle 2| \end{aligned} \tag{2.41}$$

Using the action of $\mathbf{G}$ on $\langle 2|$, $|2\rangle$ to write

$$|2\rangle = \frac{1}{b}(\mathbf{G} |1\rangle - a |1\rangle); \qquad \langle 2| = \frac{1}{b}(\langle 1| \mathbf{G} - a\langle 1|) \tag{2.42}$$

one finds

$$\begin{aligned} d_i = \frac{\alpha}{q} \Bigg[& \left(2a - b^2 - \frac{a^2}{b^2}\right) \frac{J_N}{q} \langle \sigma_{i-1} \rangle_{N-1} + \left(\frac{a}{b^2} - q - 1\right) \langle \sigma_{i-1} \rangle_N \\ & + \left(\frac{a}{b^2} - a - 1 + q\right) \langle \sigma_i \rangle_N + \frac{b^2-1}{b^2} \frac{q}{J_{N+1}} \langle \sigma_i \rangle_{N+1} \Bigg] \end{aligned} \tag{2.43}$$

where J_N is the current (2.28) in a system of size N and $\langle \sigma_i \rangle_N$ is the density of holes (2.24) at site i in a system of size N. One can see that in the power-law phase, for large i, the sum of order-i terms $\langle \sigma \rangle$ which decay like $i^{-3/2}$ will generate a decay of $i^{-1/2}$ for the particle densities. In fact one can show by a more careful calculation that

$$\langle \tau_n \rangle \simeq \begin{cases} \frac{1}{2} + \frac{1}{2\sqrt{\pi}\, n^{1/2}} + \cdots & \text{for } \frac{q}{\alpha} < (q-2)^2,\ q < 2, \text{ and } n \text{ large} \\ \frac{1}{2} + \frac{1}{2\sqrt{\pi}\, n^{1/2}} \frac{q-1}{q} + \cdots & \text{for } \frac{q}{\alpha} = (q-2)^2,\ q < 2, \text{ and } n \text{ large} \end{cases} \tag{2.44}$$

The symmetry of the model under the interchange of positive and negative particles and their directions implies that $\langle \tau_i \rangle = \langle \theta_{N-i+1} \rangle$. Using this relation and $\langle \tau_i \rangle + \langle \theta_i \rangle + \langle \sigma_i \rangle = 1$, one can obtain the densities of negative particles and decays to the bulk density from the right-hand boundary. The bulk density of positive particles is equal to the bulk density of negative particles. Thus the bulk density of positive particles is one-half in the power-law phase and can be simply obtained from (2.38) in the exponential phase.

Remark. An easy way to obtain exact expressions for quantities of interest is to note that if one defines

$$\begin{aligned} \tilde{\mathbf{D}} &= \mathbf{D} + (\gamma\alpha/q - \alpha)\, \mathbf{A} \\ \tilde{\mathbf{E}} &= \mathbf{E} + (\delta\alpha/q - \alpha)\, \mathbf{A} \end{aligned} \tag{2.45}$$

where γ and δ satisfy

$$\begin{aligned} \gamma + \delta &= 2q + q/\alpha \\ \gamma\delta &= q^2 + q/\alpha \end{aligned} \tag{2.46}$$

then one can check using the algebra (2.8)–(2.14) that

$$\begin{aligned} \tilde{\mathbf{D}}\tilde{\mathbf{E}} &= \tilde{\mathbf{D}} + \tilde{\mathbf{E}} = \mathbf{G} \\ \langle W |\, \tilde{\mathbf{E}} &= \langle W |\, \delta; \qquad \tilde{\mathbf{D}}\, | V \rangle = \gamma\, | V \rangle \end{aligned} \tag{2.47}$$

These equations are the algebra of matrices used in the solution of a one-species asymmetric exclusion process with feeding rate $1/\delta$ and removal rate $1/\gamma$.[20] Thus one can use Eq. (39) of ref. 20 to write down an exact expression for $\langle W |\, \mathbf{G}^N\, | V \rangle$,

$$\langle W |\, \mathbf{G}^N\, | V \rangle = \sum_{p=1}^{N} \frac{p(2N-1-p)!}{N!\,(N-p)!} \frac{\gamma^{p+1} - \delta^{p+1}}{\gamma - \delta} \tag{2.48}$$

Similarly one can quickly obtain exact expression for the particle densities. For example, we find from (2.45) that

$$\langle \tau_i \rangle = \langle \tilde{\tau}_i \rangle - (\gamma\alpha/q - \alpha) \langle \sigma_i \rangle \tag{2.49}$$

where $\langle \tilde{\tau}_i \rangle$ defined by

$$\langle \tilde{\tau}_i \rangle = \frac{\langle W| \mathbf{G}^{i-1} \tilde{\mathbf{D}} \mathbf{G}^{N-i} |V\rangle}{\langle W| \mathbf{G}^N |V\rangle} \tag{2.50}$$

is the density of particles in a one-species exclusion process. Then, using Eq. (43) of ref. 20 and (2.24), we find an exact expression (for $i \neq N$)

$$\begin{aligned} \langle \tau_i \rangle = & \sum_{p=0}^{N-i-1} \frac{2p!}{p!\,(p+1)!} \frac{\langle W| \mathbf{G}^{N-1-p} |V\rangle}{\langle W| \mathbf{G}^N |V\rangle} \\ & + \frac{\langle W| \mathbf{G}^{i-1} |V\rangle}{\langle W| \mathbf{G}^N |V\rangle} \sum_{p=2}^{N-i+1} \frac{(p-1)(2N-2i-p)!}{(N-i)!\,(N-i+1-p)!} \gamma^{-p} \\ & - (\gamma - q) \frac{\langle W| \mathbf{G}^{i-1} |V\rangle \langle W| \mathbf{G}^{N-i} |V\rangle}{\langle W| \mathbf{G}^N |V\rangle} \end{aligned} \tag{2.51}$$

and

$$\langle \tau_N \rangle = q \frac{\langle W| \mathbf{G}^{N-1} |V\rangle}{\langle W| \mathbf{G}^N |V\rangle} \tag{2.52}$$

In this section we have given the exact solutions for the two planes ($\alpha = \infty$) and ($\beta = 1$) in the parameter space of α, β, and q. In this way we have identified two phases: a maximal-current phase where the density

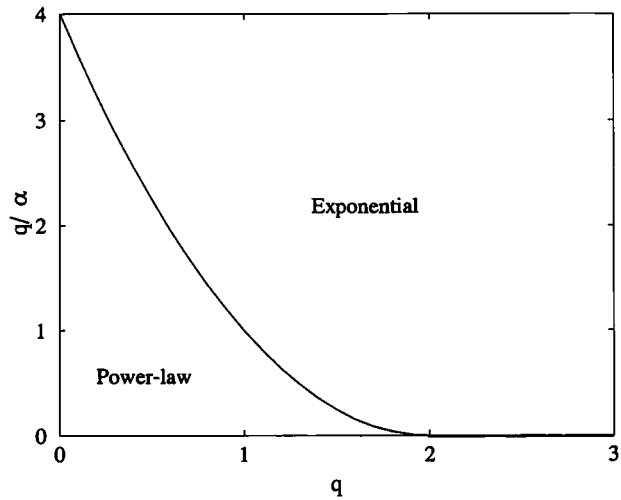

Fig. 1. The $\beta = 1$ phase diagram (exact). The transition between the power-law phase and the exponential phase is continuous. The bold line marks the line of shock configurations.

profiles decay according to a power law and an exponential phase where the density profile decays exponentially. Also we have seen that for $\alpha = \infty$ and $\beta < q/2$ the density profile is a superposition of shocks. The information given here is summarized in the phase diagram given in Fig. 1. In the next section we explore other areas of the parameter space by the use of mean-field theory and provide evidence that further phases exist. Of course it remains a challenge to find exact solutions for these cases, too.

3. MEAN-FIELD THEORY

In this section we discuss the mean-field theory of the model for general values of α, β, and q. We study in detail the $q = 1$ case, for which stationary solutions to mean-field equations may be found analytically. We then comment on some features of the phase diagram for $q \neq 1$, which may be obtained numerically.

In the mean-field approximation correlations are ignored, and pair and higher correlation functions are written as products of average occupation numbers. For example,

$$\langle \tau_i \tau_j \rangle = \langle \tau_i \rangle \langle \tau_j \rangle \tag{3.1}$$

We define the mean-field densities of positive and negative particles at site i as

$$\begin{aligned} p_i &= \langle \tau_i \rangle \\ m_i &= \langle \theta_i \rangle \end{aligned} \tag{3.2}$$

Their time evolution is given by the following equations:

$$\begin{aligned} \frac{dp_i}{dt} &= j^+_{i-1,\,i} - j^+_{i,\,i+1} \\ \frac{dm_i}{dt} &= j^-_{i+1,\,i} - j^-_{i,\,i-1} \end{aligned} \tag{3.3}$$

where the mean-field currents read

$$\begin{aligned} j^+_{i,\,i+1} &= p_i [1 - p_{i+1} - (1-q)\, m_{i+1}] \\ j^-_{i+1,\,i} &= m_{i+1} [1 - m_i - (1-q)\, p_i] \end{aligned} \tag{3.4}$$

as is found by neglecting correlations in Eqs. (2.26), (2.27). At the boundaries one has

$$\begin{aligned} j^+_{0,\,1} &= \alpha(1 - p_1 - m_1) \\ j^+_{N,\,N+1} &= \beta p_N \\ j^-_{1,\,0} &= \beta m_1 \\ j^-_{N+1,\,N} &= \alpha(1 - p_N - m_N) \end{aligned} \tag{3.5}$$

In a stationary state the currents of positive or negative particles are constant throughout the system, i.e., $j^+_{i,i+1} = j^+$ and $j^-_{i+1,i} = j^-$ for all i, and Eq. (3.4) define a mapping between the densities (p_i, m_i) at site i and those at site $i+1$. For $1 < i < N$ one has

$$\begin{aligned} j^+ &= p_i[1 - p_{i+1} - (1-q)\, m_{i+1}] \\ j^- &= m_{i+1}[1 - m_i - (1-q)\, p_i] \end{aligned} \tag{3.6}$$

whereas for the boundary sites

$$\begin{aligned} j^+ &= \alpha(1 - p_1 - m_1) = \beta p_N \\ j^- &= \beta m_1 = \alpha(1 - p_N - m_N) \end{aligned} \tag{3.7}$$

Note that in mean field there is no *a priori* reason that the two currents should be the same, even for a finite system. In the stochastic system such a breaking of the symmetry may only occur in the limit of an infinite size, due to the ergodic nature of the finite system.

3.1. Mean-Field Solution for $q = 1$

It is readily seen from Eqs. (3.6) that when $q = 1$ the two bulk equations decouple. Intuitively, the reason is that, away from the boundaries, a positive particle does not distinguish between a hole and a negative particle, and neither does a negative particle distinguish between a hole and a positive particle. At the boundaries the introduction of a particle into the system requires that there be a hole on the site of entry. The two systems of particles are therefore coupled via the boundary equations (3.7).

Defining

$$\begin{aligned} \alpha^+ &= \frac{\alpha(1 - p_1 - m_1)}{1 - p_1} = \frac{j^+}{j^+/\alpha + j^-/\beta} \\ \alpha^- &= \frac{\alpha(1 - p_N - m_N)}{1 - m_N} = \frac{j^-}{j^-/\alpha + j^+/\beta} \\ \beta^+ &= \beta^- = \beta \end{aligned} \tag{3.8}$$

reduces the problem to two one-species totally asymmetric exclusion processes on a lattice of size N. One process corresponds to the $+$ particles and the other corresponds to the $-$ particles. We then have to solve two sets of equations of the form

$$\begin{aligned} j^+ &= \alpha^+(1 - p_1) = p_1(1 - p_2) = \cdots = p_{N-1}(1 - p_N) = \beta p_N \\ j^- &= \beta m_1 = m_2(1 - m_1) = \cdots = m_N(1 - m_{N-1}) = \alpha^-(1 - m_N) \end{aligned} \tag{3.9}$$

The solutions of each separate set of equations are known[19] and read as follows where α^s, β^s, and j^s denote the feeding rate, removal rate, and current, respectively, of a single-species process:

- $\alpha^s \geqslant 1/2$ and $\beta^s \geqslant 1/2$ defines the power-law or maximal-current phase. The approach to the bulk density ($=1/2$) obeys a power law. The current is maximal with $j^s = 1/4$.
- $\alpha^s < \beta^s$ and $\alpha^s < 1/2$ defines the low-density phase. The current is $j^s = \alpha^s(1-\alpha^s)$ and the bulk density, equal to α^s, is approached exponentially.
- $\beta^s < \alpha^s$ and $\beta^s < 1/2$ defines the high-density phase. The current is $j^s = \beta^s(1-\beta^s)$ and the bulk density, equal to $1-\beta^s > 1/2$, is approached exponentially.

However, the two sets of equations (3.9) are still coupled via Eqs. (3.8), which therefore impose consistency conditions on the solutions of Eqs. (3.9).

It is possible for the system as a whole to be in a broken symmetry state if one set of particles is in one single-species phase and the other one is in another. It is clear that not all the combinations of phases are allowed. For example, it is not possible to have one particle type in the power-law phase and the other in the high-density phase, since the total bulk density of particles would then exceed one.

We shall start by studying the possible symmetric phases ($j^+ = j^-$), then we will study the possible asymmetric ones ($j^+ \neq j^-$).

3.1.1. Symmetric Phases. The two allowed symmetric phases are the power-law/power-law and the low-density/low-density phases. In these phases $j^+ = j^-$, hence

$$\alpha^s = \alpha^+ = \alpha^- = \frac{\alpha\beta}{\alpha+\beta} \tag{3.10}$$

and $p_1 = m_N$.

Power-Law Symmetric Phase. In this phase $j^s = 1/4$ and the bulk densities are $p = m = 1/2$. The conditions for the existence of this phase are

$$\alpha^s \geqslant 1/2, \qquad \beta > 1/2 \tag{3.11}$$

The second condition is guaranteed by the first one, which reads

$$\frac{\alpha\beta}{\alpha+\beta} \geqslant \frac{1}{2} \tag{3.12}$$

Low-Density Symmetric Phase. In this phase $j^s = \alpha^s(1-\alpha^s)$ and the bulk densities are $p = m = \alpha^s$. The conditions for the existence of this phase are

$$\alpha^s \leqslant 1/2, \qquad \alpha^s < \beta \tag{3.13}$$

The second condition is always satisfied and the first one reads

$$\frac{\alpha\beta}{\alpha+\beta} < \frac{1}{2} \tag{3.14}$$

From (3.12), (3.14) one can see that for all values of α and β there is a symmetric solution of the mean-field equations corresponding to one of the two symmetric phases. They correspond to the two phases found in the exact solution for $\beta = 1$. The density profiles for these two phases are given in Figs. 2a–5a. As discussed later, in checking the stability of the symmetric phases it is found that the low-density phase becomes unstable to nonsymmetric perturbations in a region of the α–β plane, giving rise to asymmetric phases. These structures are studied next.

3.1.2. Asymmetric Phases. The three types of asymmetric phases which may exist—from the simple consideration of single occupancy of sites—are the low-density/low-density, high-density/low-density, and power-law/low-density phases. It can be shown that the latter does not exist for $q = 1$; however, as the proof is rather lengthy, it will not be given here. Since the combination of power-law decays in the density of one species of particle and exponential decays for the other seems physically unlikely, we expect that such a phase would not exist even for $q \neq 1$.

High-Density/Low-Density Phase. Without loss of generality it will be assumed that the positive particles are in the high-density phase; thus we have

$$\begin{aligned} j^+ &= \beta(1-\beta) \\ j^- &= \alpha^-(1-\alpha^-) \end{aligned} \tag{3.15}$$

The densities in the bulk are $1-\beta$ and α^-. The conditions for the existence of this phase are

$$\begin{aligned} &\beta < 1/2, \qquad \beta < \alpha^+ \\ &\alpha^- < 1/2, \qquad \alpha^- < \beta \end{aligned} \tag{3.16}$$

Substituting (3.15) into Eqs. (3.8) and using the restriction that $\alpha^- < 1/2$, we find

$$\alpha^- = \frac{1+\alpha}{2} - \frac{1}{2}[(1+\alpha)^2 - 4\alpha\beta]^{1/2} \tag{3.17}$$

The current j^- and the feeding rate α^+ may then be deduced from Eqs. (3.15), (3.8).

The conditions given in Eq. (3.16) define the region of existence of the high-density-low-density asymmetric phase in the α–β plane. It is found that this region is uniquely determined by only one of these conditions, namely

$$\alpha^+ > \beta \tag{3.18}$$

See Fig. 6 and the discussion at the end of this section. Note that in this phase the current j^+ is larger than j^-, since $\alpha^- < \beta$.

Low-Density/Low-Density Asymmetric Phase. In this phase

$$\begin{aligned} j^+ &= \alpha^+(1-\alpha^+) \\ j^- &= \alpha^-(1-\alpha^-) \end{aligned} \tag{3.19}$$

The densities in the bulk are α^+ and α^-. Without loss of generality we take $\alpha^+ > \alpha^-$, which implies that $j^+ > j^-$. Substituting into Eqs. (3.8), we find the following equations for α^+ and α^-:

$$\begin{aligned} \alpha^+ &= 1 - \frac{1}{\alpha}\alpha^+(1-\alpha^+) - \frac{1}{\beta}\alpha^-(1-\alpha^-) \\ \alpha^- &= 1 - \frac{1}{\beta}\alpha^+(1-\alpha^+) - \frac{1}{\alpha}\alpha^-(1-\alpha^-) \end{aligned} \tag{3.20}$$

A simple way to solve these equations is to define

$$S = \alpha^+ + \alpha^-; \qquad D = \alpha^+ - \alpha^- \tag{3.21}$$

Taking the difference of equations appearing in (3.20), and using the definitions of S and D, we find

$$D = \left(\frac{\alpha-\beta}{\alpha\beta}\right) D(1-S) \tag{3.22}$$

In order to have an asymmetric phase we require $D \neq 0$, hence

$$S = 1 - \frac{\alpha\beta}{\alpha-\beta} \tag{3.23}$$

Summing the equations appearing in (3.20) leads to

$$D=\left[(S-2)\left(\frac{2\alpha\beta}{\alpha+\beta}-S\right)\right]^{1/2} \tag{3.24}$$

The values for the currents follow directly:

$$\begin{aligned} j^{+} &= \tfrac{1}{4}(S+D)(2-S-D) \\ j^{-} &= \tfrac{1}{4}(S-D)(2-S+D) \end{aligned} \tag{3.25}$$

and the bulk densities α^{+} and α^{-} are equal to the half of the sum and difference of S and D, respectively.

The conditions for the existence of this phase are

$$\begin{aligned} &\alpha^{+}<1/2, \qquad \alpha^{+}<\beta \\ &\alpha^{-}<1/2, \qquad \alpha^{-}<\beta \end{aligned} \tag{3.26}$$

These conditions define a region of the α–β plane which is uniquely determined by only one of them, namely

$$\alpha^{+}<\beta \tag{3.27}$$

Comparing this last equation with Eq. (3.18), we see that on increasing β the transition from the high-density/low-density phase to the low-density/low-density asymmetric phase occurs when $\alpha^{+}=\beta$. This condition corresponds to a shock for the phase of higher density (see the comments on Figs. 2a–5a below).

An additional condition for the existence of the low-density/low-density asymmetric phase is that D be real. This is indeed the case as long as (3.27) is satisfied. At the transition to the low-density symmetric phase, D vanishes. This occurs either when $S=2$, which is excluded since it would lead to bulk densities larger than 1/2, or when

$$S=\frac{2\alpha\beta}{\alpha+\beta} \tag{3.28}$$

This relation together with (3.23) yield the following expression for α^{s} on the transition line between the low-density/low-density asymmetric phase and the low-density symmetric phase:

$$\alpha^{+}=\alpha^{-}=\frac{\alpha\beta}{\alpha+\beta}=\frac{1}{2}\left(1-\frac{\alpha\beta}{\alpha-\beta}\right) \tag{3.29}$$

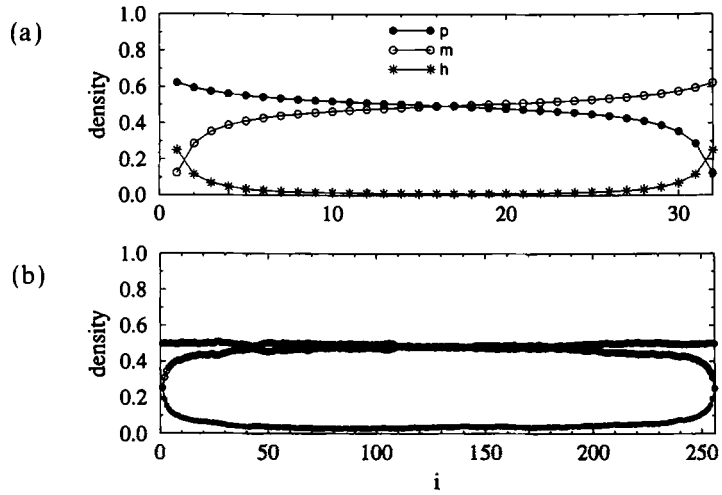

Fig. 2. (a) Mean-field profiles for the power-law symmetric phase ($\alpha = 1$, $\beta = 2$, $q = 1$), $N = 32$. (b) Monte Carlo profiles for the power-law symmetric phase ($\alpha = 1$, $\beta = 2$, $q = 1$), $N = 256$.

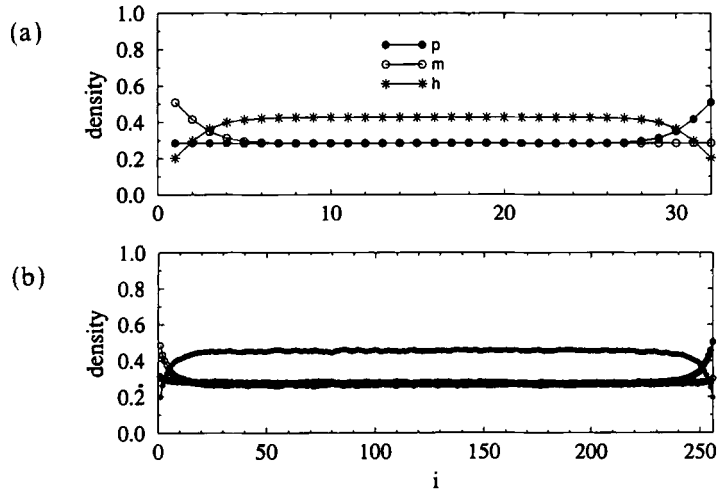

Fig. 3. (a) Mean-field profiles for the low-density symmetric phase ($\alpha = 1$, $\beta = 0.4$, $q = 1$). (b) Monte Carlo profiles for the low-density symmetric phase ($\alpha = 1$, $\beta = 0.4$, $q = 1$).

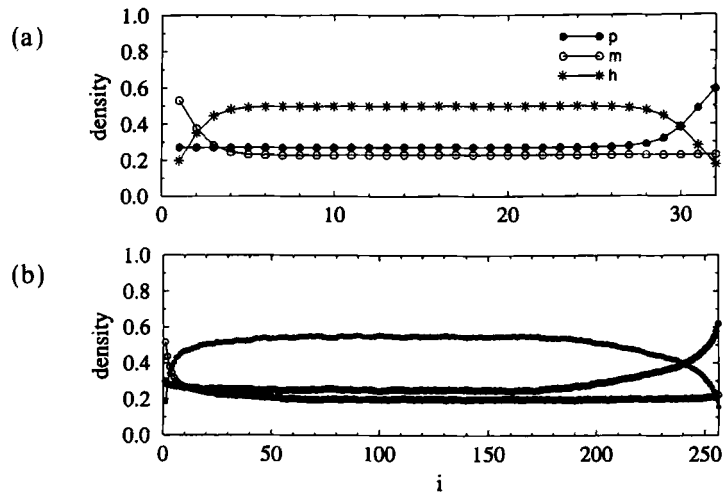

Fig. 4. (a) Mean-field profiles for the low-density/low-density asymmetric phase ($\alpha = 1$, $\beta = 0.333$, $q = 1$). (b). Monte Carlo profiles for the low-density asymmetric phase ($\alpha = 1$, $\beta = 0.3$, $q = 1$).

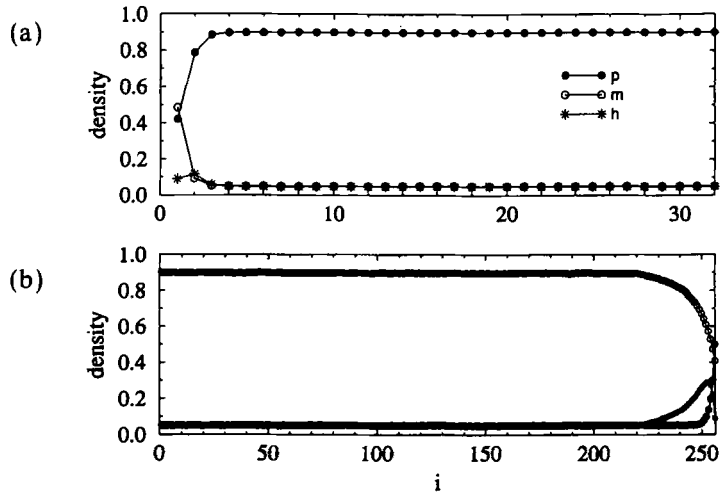

Fig. 5. (a) Mean-field profiles for the high-density/low-density asymmetric phase ($\alpha = 1$, $\beta = 0.1$, $q = 1$). (b) Monte Carlo profiles for the high-density/low-density asymmetric phase ($\alpha = 1$, $\beta = 0.1$, $q = 1$).

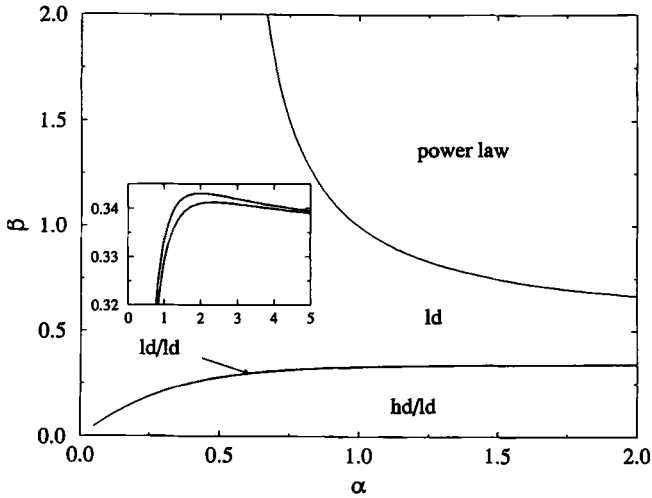

Fig. 6. Phase diagram for the case $q = 1$ (mean field). The inset shows the two lines of transition defining the low-density/low-density phase.

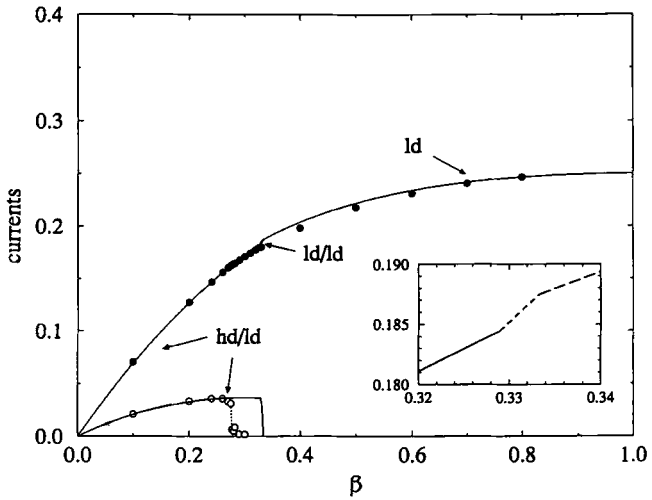

Fig. 7. Currents $[(j^+ + j^-)/2$ and $|j^+ - j^-|/2]$ against β for $q = 1$, $\alpha = 1$. Mean-field: continuous lines. Monte Carlo: $(j^+ + j^-)/2$, filled circles; $|j^+ - j^-|/2$, open circles. The inset is a detail of the region of transitions. Only $(j^+ + j^-)/2$ is given.

Typical density profiles corresponding to the two asymmetric phases are given in Figs. 2a–5a, which correspond to $\alpha = 1$ and $\beta = 2$, 0.4, 0.333, and 0.1 for a system size $N = 32$. Some comments are in order. In Fig. 5a, the bulk density of the phase of lower density (m here) is equal to α^-, whereas the bulk density of the phase of higher density (p) is equal to $1-\beta$. When β increases, α^- increases. The transition from the high-density/low-density phased to the low-density/low-density asymmetric phase is reached when $\beta = \alpha^+ = 0.328956$. On the transition line one species of particles (here the positive particles) display coexistence between a phase of higher density $1-\beta$ and a phase of lower density α^+. A typical configuration of the positive charges is thus composed of a density profile with a localized shock separating the two densities.

Above this transition the bulk density of the phase of higher density is equal to α^+. This is the case in Fig. 4a. The transition of this asymmetric phase to the low-density symmetric phase is reached when the two bulk densities α^+ and α^- are equal, i.e., when $\beta = 1/3$.

In summary, the phase diagram for $q = 1$ is given in Fig. 6, where we see four regions: the power-law symmetric phase, the low-density symmetric phase, the low-density/low-density asymmetric phase, and the high-density/low-density asymmetric phase. The behavior of the two currents along the $\alpha = 1$ line is given in Fig. 7. Note that although the low-density symmetric phase exists throughout the regions of existence of the nonsymmetric solutions, it becomes unstable to nonsymmetric perturbations. This can easily been checked numerically, at least for a finite system, by linearizing the dynamical equations (3.3) around the low-density symmetric phase. The real part of one of the eigenvalues of the evolution matrix becomes positive at a point approaching the transition line (3.29) as N becomes large. The difference of currents $j^+ - j^-$ behaves as $(\beta_c - \beta)^{1/2}$ near the transition.

For the sake of clarity we regroup here the equations of the three lines of transitions seen on Fig. 6.

- From the power-law region to the low-density symmetric region:

$$\frac{\alpha\beta}{\alpha+\beta} = \frac{1}{2} \tag{3.30}$$

- From the low-density symmetric region to the low-density/low-density asymmetric region:

$$\frac{\alpha\beta}{\alpha+\beta} = \frac{1}{2}\left(1 - \frac{\alpha\beta}{\alpha-\beta}\right) \tag{3.31}$$

• From the low-density/low-density asymmetric region to the high-density/low-density asymmetric region:

$$\alpha^+ = \beta \tag{3.32}$$

where α^+ may be determined by Eqs. (3.8) and (3.17).

Note that all three lines represent continuous transitions.

3.2. The Case $q \neq 1$

The complete phase diagram of the model in the (α, β, q) parameter space may be rather complex. We did not study this phase diagram in detail. However, we would like to comment briefly on some of its features for $q \neq 1$. In particular, we examine in some detail the phase transition between the two symmetric phases: the power-law and the low-density ones.

Let us consider first the possible bulk densities of the two types of particles. These densities may be obtained from Eqs. (3.6) with periodic boundary conditions. For the symmetric phases one has to take $j^+ = j^- = j$. One finds that these equations have two types of solutions, one with $p = m$ and the other with $p + m = 1$. It can be shown that the latter solution is only relevant in the $\alpha = \infty$ limit. Here we are interested in the $p = m$ solution, for which we have

$$p = m = \frac{1 \pm [1 - 4j(2-q)]^{1/2}}{2(2-q)} \tag{3.33}$$

and

$$j = p(1-2p) + qp^2 \tag{3.34}$$

To this solution, the condition $p \leqslant 1/2$ needs to be added, giving rise to two distinct behaviors for $q < 1$ and $q > 1$. For $q > 1$ the current is a monotonically increasing function of p. It reaches its maximum $j = q/4$ at $p = m = 1/2$ corresponding to the power-law phase. For $p < 1/2$ the corresponding phase is the low-density one. On the other hand, for $q < 1$ the $j(p)$ curve exhibits a maximum for $p = 1/[2(2-q)]$, $j = 1/[4(2-q)]$. Again, the curve terminates at $j = q/4$ for $p = m = 1/2$, corresponding to the power-law phase.

Returning to the open chain, we consider the current $j(\alpha)$ and the bulk density $p(\alpha)$ for fixed β and q. For $q > 1$, j and p increase with α. At some critical α the current reaches its maximal value $j = q/4$ and a continuous transition to the power-law phase takes place.

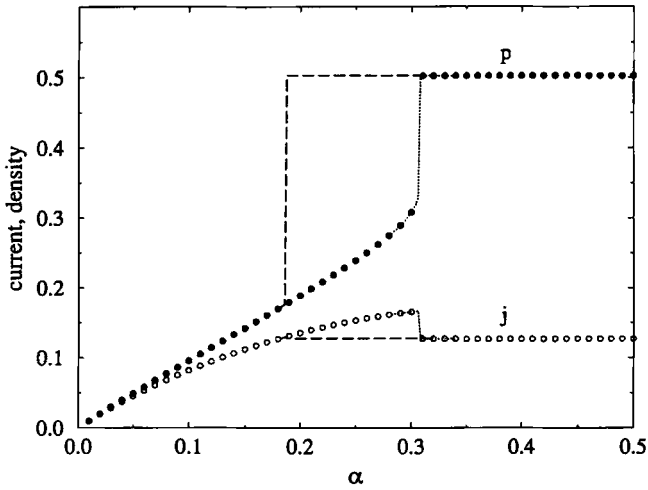

Fig. 8. Current and density in mean field for $q = 0.5$, $\beta = 1$, and $N = 32$, as a function of α. The circles correspond to the initial condition $p = m < 0.5$, whereas the long-dashed curves correspond to the initial condition $p = m = 0.5$. Open circles represent the current, filled ones the density. Small dots correspond to continuation of the curves, with a smaller increment in α. Hysteretic behavior is clearly seen.

On the other hand, the behavior of the $q < 1$ case is quite different. For small α there is a stable low-density phase. The current j and the bulk density p increase as α is increased. However, before j reaches its maximal value, $j = 1/[4(2-q)]$, the power-law solution corresponding to $p = m = 1/2$ and $j = q/4$ becomes locally stable. The system thus has two locally stable solutions: a low-density and a power-law phase. This results in a first-order transition, as can be seen in Fig. 8. One can compare the mean-field result for $\beta = 1$ with the exact solution obtained in Section 2. In the exact solution, the power-law/low-density transition is continuous for any q. The order of the transition is therefore wrongly predicted by the mean-field approximation. It would be interesting to study the nature of the transitions for $\beta \neq 1$ beyond the mean-field approximation.

To conclude this section, let us mention the presence of broken symmetry phases in mean field for values of $q \neq 1$.

4. MONTE CARLO SIMULATIONS

In order to check that broken symmetric phases exist in the stochastic model and to verify the general features of the phase diagram obtained by the mean-field approximation, we carried out Monte Carlo simulations of the model.

The method used for the simulations follows closely the definition of the dynamics given in Section 2. Density profiles are obtained by averaging the occupations of each site over the simulation; densities of each species ρ_+ and ρ_- by taking the mean of the profiles over all sites. The currents are defined by

$$J^{\pm} = \frac{N_{\pm}}{(N+1)\,N_{\mathrm{st}}} \tag{4.1}$$

where $N_{\pm}$ is the total number of positive (negative) particles which have moved in N_{st} Monte Carlo steps/site on a lattice of N sites. For symmetric phases, these quantities are well defined. Figures 2b and 3b show the density profiles of the two symmetric phases.

The existence of nonsymmetric phases may be identified as follows. For well-chosen parameters, e.g., $\alpha = q = 1$ and $\beta = 0.1$, one observes that the finite-size system flips in time between two states: one in which $\rho_+ = \rho_1$, $J^+ = j_1$, $\rho_- = \rho_2$, $J^- = j_2$, the other one, symmetric to the former, such that $\rho_+ = \rho_2$, $J^+ = j_2$, $\rho_- = \rho_1$, $J^- = j_1$.

The flipping time $\tau(N)$ between these equivalent nonsymmetric phases increases as the system size increases. Numerical studies of $\tau(N)$ for $N \leqslant 160$ suggest that $\tau(N)$ increases exponentially with N,[23] indicating that spontaneous symmetry breaking takes place.

Therefore, for a fixed system size N, when time increases, all quantities defined above (profiles, densities, and currents) should appear progressively symmetric, i.e., equal for the two species. The right quantities to measure should therefore be symmetric combinations of these, such as the sum and absolute difference of densities or currents. Furthermore, a finite-size analysis would be required in order to get accurate quantitative estimates of these quantities, especially when approaching the transition to the symmetric phase, for $\beta \approx 0.3$ in the case $\alpha = q = 1$ considered here.

Instead, in order to have a quick illustration of the presence of broken symmetric phases we measured the profiles, densities, and currents for each species, taking the time of the simulation small compared to the flipping time $\tau(N)$. This procedure is good when β is small enough, but becomes more problematic when approaching the transition $\beta \to \beta_c$. The results found for this region are therefore just indicative.

Let us give some comments on Figs. 2b–5b. They show qualitatively the same behavior as the corresponding Figs. 2a–5a found in the mean-field approximation. A noticeable difference between the stochastic model and its mean-field approximation are the behaviors of the decays of the density profiles at the boundaries, as in the one-species case.[19] Figure 7 shows $(J^+ + J^-)/2$ and $|J^+ - J^-|/2$ for $q = 1$, $\alpha = 1$ plotted against β for a system

of 256 sites. Note the overall striking agreement between the values of these quantities obtained in simulations with those of the mean-field theory.

As in mean field we checked the presence of broken symmetry phases for values of $q \neq 1$.

5. CONCLUSION

In the present work we studied a simple one-dimensional driven diffusive process for two species which exhibits *spontaneous symmetry breaking*. This is an asymmetric exclusion model of two oppositely charged particles driven by an electric field on an open chain. The positively charged particles are supplied at the left end and they leave the system at the right end. Similarly, the negatively charged particles are supplied at the right end and they leave the system at the left end. The system is invariant under charge conjugation combined with space inversion. The model is studied using the mean-field approximation and Monte Carlo simulations. Its steady-state properties can also be studied exactly in a certain limited range of the parameter space defining its dynamics. This may be done by the matrix method which was recently introduced.[20] Beyond symmetric phases, two phases in which the currents of the positive and negative charges are different from each other are found, suggesting that spontaneous symmetry breaking takes place. These phases exist for values of the parameters outside the region where the exact solution was obtained. It would be interesting to know whether exact solutions could be found using matrix methods for any values of the parameters defining the model, and in particular in the region in which symmetry breaking does take place. Extensions of the present study to higher dimensions would also be of interest.

We conclude by showing how the model we have studied may also be viewed as describing an evolution process of a moving interface. To demonstrate this point consider a one-dimensional solid-on-solid model and let h_i be the height variable at site i ($i = 1,..., N$). The heights take integer values with the restriction that the heights of nearest-neighbor sites do not differ by more than 1. During an infinitesimal time interval dt, each bulk site i ($i = 2,..., N-1$) is updated according to the following rule: the height is increased by $l = 1, 2$ with probability $W_i(h_{i-1}(t), h_i(t), h_{i+1}(t); l)\, dt$. The probability per unit time takes the form

$$W_i(h_{i-1}(t), h_i(t), h_{i+1}(t); 1) = \begin{cases} 1 & \text{for } h_{i+1} = h_i = h_{i-1} - 1 \text{ or } h_{i-1} = h_i = h_{i+1} - 1 \\ 0 & \text{otherwise} \end{cases} \tag{5.1}$$

$$W_i(h_{i-1}(t), h_i(t), h_{i+1}(t); 2) = \begin{cases} q & \text{for } h_{i+1} = h_{i-1} = h_i + 1 \\ 0 & \text{otherwise} \end{cases} \tag{5.2}$$

The end sites $i=1$ and $i=N$ are updated by a different rule. They are increased by 1 with probability $W_1(h_1(t), h_2(t))\,dt$ and $W_N(h_{N-1}(t), h_N(t))\,dt$, respectively.

The W's take the form

$$W_1(h_1(t), h_2(t)) = \begin{cases} \alpha & h_1 = h_2 \\ \beta & h_1 = h_2 - 1 \\ 0 & \text{otherwise} \end{cases} \tag{5.3}$$

$$W_N(h_{N-1}(t), h_N(t)) = \begin{cases} \alpha & h_N = h_{N-1} \\ \beta & h_N = h_{N-1} - 1 \\ 0 & \text{otherwise} \end{cases} \tag{5.4}$$

It is easy to see that this growth model is equivalent to the two-species asymmetric exclusion model by identifying $h_i - h_{i+1} = 1, 0, -1$ with a positive particle, a vacancy, and a negative particle, respectively.

Thus one can think of a configuration of particles on the lattice as representing an interface composed of terraces. The interface grows by the steps at the edge of the terraces moving in from the boundaries: the dynamics of a positive particle corresponds to a step moving in from the left boundary and the dynamic of a negative particle corresponds to a step moving in from the right boundary. When two steps moving in opposite directions meet, a new terrace, and thus two new steps, are nucleated with rate q.

This growth model is closely related to the one recently studied in refs. 8 and 13. The main difference is that in the present model, the evolution of the bulk sites [Eqs. (5.1)–(5.4)] has two conserved quantities (the number of upward and the number of downward steps), while in the previous model only the difference between the upward and the downward steps is conserved.

In terms of the growth model the phases we have studied have natural interpretations. The symmetric phases correspond to power-law or exponential decay of the interface height to a flat interface far away from the boundaries. The line of shocks corresponds to V-shaped surface configurations. The symmetry-breaking transitions correspond to the interface spontaneously acquiring a slope: either a large slope in the case of the high-density/low-density phase or a weak slope in the case of the low-density/low-density phase.

APPENDIX A. PROOF OF MATRIX ALGEBRA (2.8)–(2.14)

Here we prove the matrix algebra (2.8)–(2.14), which allows us to obtain the exact solution of the model in the case $\beta = 1$. The proof we give here is based on that given in ref. 20. Let us begin by writing down the master equation:

$$\begin{aligned}\frac{d}{dt} P_N(s_1, s_2, \ldots, s_N) &= \sum_{s_1'} (h_1)_{s_1; s_1'} P_N(s_1', s_2, \ldots, s_N) \\ &+ \sum_{i=1}^{N-1} \sum_{s_i', s_{i+1}'} (h)_{s_i, s_{i+1}; s_i', s_{i+1}'} P_N(s_1, \ldots, s_i', s_{i+1}', \ldots, s_N) \\ &+ \sum_{s_N'} (h_N)_{s_N; s_N'} P_N(s_1, \ldots, s_{N-1}, s_N') \end{aligned} \tag{A1}$$

Here $s_i = -1, 0, 1$ and labels the state of site i. The elements of the matrices h_1, h, h_N represent the transition rates into configurations (off-diagonal elements) and out of configurations (diagonal elements). Thus

$$(h_1)_{s_1; s_1'}$$

is the transition rate from a configuration with the first site in state s_1' to a configuration identical except that the first site is in state s_1, i.e., h_1 represents transitions due to events at the left-hand boundary. Similarly h represents transitions due to the particles hopping between two non-boundary sites and h_N represents transitions due to events at the right-hand boundary. One can easily construct these matrices and one finds that the only nonzero elements are

$$\begin{aligned}(h_1)_{1;0} &= -(h_1)_{0;0} = \alpha \\ (h_1)_{0;-1} &= -(h_1)_{-1;-1} = 1 \\ (h)_{-1,0;0,-1} &= -(h)_{0,-1;0,-1} = 1 \\ (h)_{0,1;1,0} &= -(h)_{1,0;1,0} = 1 \\ (h)_{-1,1;1,-1} &= -(h)_{1,-1;1,-1} = q \\ (h_N)_{-1,0} &= -(h_1)_{0;0} = \alpha \\ (h_N)_{0;1} &= -(h_N)_{1;1} = 1 \end{aligned}$$

The fact that the elements of each column of all the transition matrices add up to zero simply reflects the conservation of probability.

Now let us assume that there exist three coefficients x_{-1}, x_0, x_1, such that the following conditions on the weights f_N (where $P_N = f_N/Z_N$ and Z_N is the normalization, which is independent of configuration) are satisfied for each choice of s_i:

$$\sum_{s_1'} (h_1)_{s_1; s_1'} f_N(s_1', s_2, \ldots, s_N) = x_{s_1} f_{N-1}(s_2, \ldots, s_N) \tag{A2}$$

$$\sum_{s_i', s_{i+1}'} (h)_{s_i, s_{i+1}; s_i', s_{i+1}'} f_N(s_1, \ldots, s_i', s_{i+1}', \ldots, s_N) = -x_{s_i} f_{N-1}(s_1, \ldots, s_{i-1}, s_{i+1}, \ldots, s_N) + x_{s_{i+1}} f_{N-1}(s_1, \ldots, s_i, s_{i+2}, \ldots, s_N) \tag{A3}$$

$$\sum_{s_N'} (h_N)_{s_N; s_N'} f_N(s_1, \ldots, s_{N-1}, s_N) = -x_{s_N} f_{N-1}(s_1, \ldots, s_{N-1}) \tag{A4}$$

If such coefficients x_{-1}, x_0, x_1 exist, then the f_N (or P_N) given by the equalities (A2)–(A4) are automatically steady state quantities $[(d/dt)\, P_N = 0]$, since on substituting (A2)–(A4) into (A1), the rhs of (A1) is zero. When we replace f_N by their expressions (2.1)–(2.3) and substitute into (A2)–(A4), we obtain the following conditions:

$$\begin{aligned} 0 &= x_{-1} + x_0 + x_1 \\ \alpha \langle W| A &= x_1 \langle W| \\ \langle W| E &= -x_{-1} \langle W| \\ DA &= x_1 A - x_0 D \\ AE &= -x_{-1} A + x_0 E \\ qDE &= x_1 E - x_{-1} D \\ \alpha A\, |V\rangle &= -x_{-1}\, |V\rangle \\ D\, |V\rangle &= x_1\, |V\rangle \end{aligned}$$

which are the same as (2.8)–(2.14) when

$$x_0 = 0; \qquad x_1 = q; \qquad x_{-1} = -q \tag{A5}$$

We note that if one tries to repeat the argument outlined above for general β, then one finds a set of algebraic rules which are inconsistent except when $\beta = 1$.

APPENDIX B. CALCULATION OF ASYMPTOTIC FORMS OF $\langle W| G^n |V\rangle$

The first step in calculating the matrix element $\langle W| G^n |V\rangle$ is to diagonalize the matrix G of (2.29), (2.30), requiring a solution of the eigenvalue equation

$$G|\phi\rangle = \lambda_\phi |\phi\rangle \tag{B1}$$

Generically the eigenvectors are of two types, a bound-state vector of the form

$$|\phi_b\rangle = \begin{pmatrix} \Delta_b \\ x \\ x^2 \\ x^3 \\ \vdots \end{pmatrix} \tag{B2}$$

with $0 \leqslant x \leqslant 1$, and an unbound-state eigenvector of the form

$$|\phi_u\rangle = \begin{pmatrix} \Delta_u \\ \cos(\theta+\mu) \\ \cos(2\theta+\mu) \\ \cos(3\theta+\mu) \\ \vdots \end{pmatrix} \tag{B3}$$

Let us start by looking at the bound-state eigenvector. By substituting $|\phi_b\rangle$ back into the eigenvalue equation (B1) we find the following conditions on Δ_b and x:

$$\Delta_b = \frac{1}{[q(2-q)]^{1/2}} \tag{B4}$$

$$(1-q)^2 x^2 + [2(1-q) - q/\alpha]\, x + 1 = 0 \tag{B5}$$

with a corresponding eigenvalue

$$\lambda_b = (1+x)^2/x \tag{B6}$$

From the conditions on x given in Eq. (B5) it may be been that there can at most be two distinct bound-state eigenvalues.

For the unbound eigenvalues the equivalent conditions are

$$\Delta_u = \frac{\cos \mu}{[q(2-q)]^{1/2}} \tag{B7}$$

with

$$\tan \mu = \frac{[q/\alpha + 2(q-1)] + [q(2-q)-2]\cos\theta}{q(2-q)\sin\theta} \tag{B8}$$

There are an infinite number of possible eigenvectors which satisfy these conditions, giving rise to a continuum of eigenvalues $\lambda_u(\theta)$ indexed by θ:

$$\lambda_u(\theta) = 2(1+\cos\theta) \tag{B9}$$

The most general solution to $\langle 1|\, G^n\, |1\rangle$ in terms of these unnormalized eigenvectors is

$$\langle 1|\, G^n\, |1\rangle = \Gamma_1^2 \lambda_{b,1}^n \langle 1|\phi_{b,1}\rangle\langle\phi_{b,1}|1\rangle + \Gamma_2^2 \lambda_{b,2}^n \langle 1|\phi_{b,2}\rangle\langle\phi_{b,2}|1\rangle + \int_{-\pi}^{\pi} \frac{d\theta}{\pi} \lambda_u^n(\theta)\langle 1|\phi_u(\theta)\rangle\langle\phi_u(\theta)|1\rangle \tag{B10}$$

where Γ_1, Γ_2 are normalization constants for the bound eigenvectors, to be calculated.

From Eq. (B5) and the condition on x it is found that the following numbers of bound-state eigenvectors exists:

No bound states when

$$\frac{q}{\alpha} \leqslant (2-q)^2 \qquad \text{and} \qquad q < 2 \tag{B11}$$

One bound state when

$$\frac{q}{\alpha} > (2-q)^2 \tag{B12}$$

Two bound states when

$$\frac{q}{\alpha} \leqslant (2-q)^2 \qquad \text{and} \qquad q > 2 \tag{B13}$$

We shall look in turn at the solutions with no, one, and two bound-state eigenvectors.

When there are no bound-state eigenvectors [$q/\alpha \leqslant (2-q)^2$ and $q<2$]

$$\langle 1|\, G^n \,|1\rangle$$

$$= \int_{-\pi}^{\pi} \frac{d\theta}{\pi} 2^n (1+\cos\theta)^n \frac{\cos^2\mu}{q(2-q)}$$

$$= \int_{-\pi}^{\pi} \frac{d\theta}{\pi} \frac{2^n q(2-q)\sin^2\theta(1+\cos\theta)^n}{q^2(2-q)^2\sin^2\theta + [q/\alpha + 2(q-1)(1+\cos\theta) - q^2\cos\theta]^2} \tag{B14}$$

This integral is solved in the limit of large n, using the saddle-point method, giving

$$\langle 1|\, G^n \,|1\rangle \simeq \begin{cases} \dfrac{q(2-q)\,4^{n+1}}{[(q-2)^2 - q/\alpha]^2\,\pi^{1/2} n^{3/2}}, & \dfrac{q}{\alpha} \neq (q-2)^2 \\ \dfrac{4^{n+1}}{2q(2-q)\,\pi^{1/2} n^{1/2}}, & \dfrac{q}{\alpha} = (q-2)^2 \end{cases} \tag{B15}$$

Considering now the region $q/\alpha > (q-2)^2$, where there is one bound-state solution with

$$x = \frac{2(q-1) + q/\alpha - \{[2(q-1)+q/\alpha]^2 - 4(1-q)^2\}^{1/2}}{2(1-q)^2} \tag{B16}$$

and the normalization Γ_1^2 given by

$$\Gamma_1^2 = \frac{q(2-q)(1-x^2)}{1-(1-q)^2 x^2} \tag{B17}$$

it may be readily seen that

$$\langle 1|\, G^n \,|1\rangle \approx \lambda_b^n \left\{ \frac{\Gamma_1^2}{q(2-q)}\, 1 + \left(\frac{4}{\lambda_b}\right)^n \frac{4\alpha^2 q(2-q)}{[q-\alpha(2-q)^2]^2\,\pi^{1/2} n^{3/2}} \right\} \tag{B18}$$

From Eq. (B18), if $q<2$, then $\langle 1|\, G^n \,|1\rangle$ approaches its limiting value from above, while if $q>2$, it does so from below. This is reflected in the density profiles for the holes, where the density is found to decrease from the boundaries to the bulk value for $q<2$ and increases to its bulk value if $q>2$.

The last region of interest is when $q>2$ and $q/\alpha < (2-q)^2$. Here there are two bound-state solutions with eigenvectors having values of x corresponding to the two solutions of Eq. (B5). Let the x corresponding to the

largest eigenvector be x_1 that corresponding to the second largest eigenvector be x_2. Both eigenvectors will have a normalization given by Eq. (B17). From Eq. (B5) it may be seen that $(1-b^2)\,x_1 x_2 = 1$, which gives

$$\Gamma_1^2 = \frac{q(2-q)(1-x_1^2)}{(1-q)^2\,(x_1 x_2 - x_1^2)} \tag{B19}$$

$$\Gamma_2^2 = \frac{q(2-q)(1-x_1^2)}{(1-q)^2\,(x_1 x_2 - x_2^2)} \tag{B20}$$

When $q > 2$, Γ_1^2 is positive, but Γ_1^2 is negative, since $x_1 > x_2$. This gives

$$\langle 1|\, G^n\, |1\rangle \approx \lambda_{b,1}^n \frac{\Gamma_1^2}{q(2-q)} \left\{ 1 - \left| \frac{\Gamma_2^2}{\Gamma_1^2} \right| \left(\frac{\lambda_{b,2}}{\lambda_{b,1}} \right)^n + \left(\frac{4}{\lambda_{b,1}} \right)^n \frac{4\alpha^2 q^2 (2-q)^2}{2[q-\alpha(2-q)^2]^2\, \pi^{1/2} n^{3/2}} \right\} \tag{B21}$$

Again it is seen that since $q > 2$, $\langle 1|\, G^n\, |1\rangle$ approaches its limiting value from below, and hence the corresponding density profile for holes will attain its bulk value from below.

ACKNOWLEDGMENTS

We thank B. Derrida, E. Domany, J. Miller, J. M. Luck, and G. Speer for interesting discussions. D.M. would like to acknowledge support from Minerva Foundation, Münich, Germany.

REFERENCES

1. S. Katz, J. L. Lebowitz, and H. Spohn, Nonequilibrium steady states of stochastic lattice gas models of fast ionic conductors, *J. Stat. Phys.* **34**:497 (1984).
2. H. Spohn, *Large Scale Dynamics of Interacting Particles* (Springer-Verlag, New York, 1991).
3. B. Schmittmann and R. K. P. Zia, Statistical mechanics of driven diffusive systems, in *Phase Transitions and Critical Phenomena*, C. Domb and J. Lebowitz, eds. (Academic, London, 1994).
4. P. Meakin, P. Ramanlal, L. M. Sander and R. C. Ball, Ballistic deposition on surfaces, *Phys. Rev.* **A34**:5091–5103 (1986).
5. J. Kertész and D. E. Spohn *Phys. Rev. Lett.* **62**:2571 (1989).
6. J. Krug and H. Spohn, Anomalous fluctuations in the driven and damped sine-Gordon chain, *Europhys. Lett.* **8**:219–224 (1989).
7. J. Krug and H. Spohn, in *Solids far from Equilibrium*, C. Godrèche ed. (Cambridge University Press, Cambridge, 1991).
8. D. Kandel and D. Mukamel, Defects, interface profile and phase transitions in growth models, *Europhys. Lett.* **20**:325–329 (1992).

9. T. M. Liggett, *Interacting Particle Systems* (Springer-Verlag, New York, 1985).
10. B. Schmittmann, K. Hwang, and R. K. P. Zia, Onset of spatial structures in biased diffusion of two species, *Europhys. Lett.* **19**:19 (1992).
11. D. P. Foster and C. Godrèche, Finite-size effects for phase segregation in a two-dimensional asymmetric exclusion model with two species, *J. Stat. Phys.* **76**:1169 (1994).
12. J. Krug, Boundary-induced phase transitions in driven diffusive systems, *Phys. Rev. Lett.* **67**:1882–1885 (1991).
13. D. Kandel, G. Gershinsky, D. Mukamel, and B. Derrida, Phase transitions induced by a defect in a growing interface model, *Physica Scripta* **T49**:622 (1993).
14. E. D. Andjel, M. Bramson, and T. M. Liggett, Shocks in the asymmetric simple exclusion process, *Prob. Theory Rel. Fields* **78**:231–247 (1988).
15. A. DeMasi, C. Kipnis, E. Presutti, and E. Saada, Microscopic structure at the shock in the simple asymmetric exclusion process, *Stochastics Stochastics Rep.* **27**:151–165 (1988).
16. P. A. Ferrari, C. Kipnis, and E. Saada, Microscopic structure traveling waves for asymmetric simple exclusion process, *Ann. Prob.* **19**:226–244 (1991).
17. C. Boldrighini, G. Cosimi, S. Frigio, and M. G. Nuñes, Computer simulation of shock waves in the completely asymmetric simple exclusion process, *J. Stat. Phys.* **55**:611-623 (1989).
18. S. A. Janowsky and J. L. Lebowitz, Finite-size effects and shock fluctuations in the asymmetric simple-exclusion process, *Phys. Rev.* **A45**:618–625 (1992).
19. B. Derrida, E. Domany, and D. Mukamel, An exact solution of a one dimensional asymmetric exclusion model with open boundaries, *J. Stat. Phys.* **69**:667–687 (1992).
20. B. Derrida, M. R. Hakim, V. Evans, and V. Pasquier, Exact solution of a 1D asymmetric exclusion model using a matrix formulation, *J. Phys. A: Math. Gen.* **26**:1493–1517 (1993).
21. G. Schütz, and E. Domany, Phase transitions in a exactly soluble one-dimensional exclusion process, *J. Stat. Phys.* **72**:277–296 (1993).
22. B. Derrida, S. A. Janowsky, J. L. Lebowitz, and E. R. Speer, Microscopic-shock profiles: Exact solution of a non-equilibrium system, *Europhys. Lett.* **22**:651–656 (1993); Exact solution of the totally asymmetric simple exclusion process: Shock profiles, *J. Stat. Phys.* **73**:813 (1993).
23. M. R. Evans, D. P. Foster, C. Godrèche, and D. Mukamel, Spontaneous symmetry breaking in a one-dimensional driven diffusive system, *Phys. Rev. Lett.* **74**:208–211 (1995).
24. M. Rubinstein, Discretized model of entangled-polymer dynamics, *Phys. Rev. Lett.* **59**:1496–1949 (1987).
25. T. A. J. Duke, Tube model of field-inversion electrophoresis, *Phys. Rev. Lett.* **62**:2877-2880 (1989).
26. B. Widom, J. L. Viovy, and A. D. Defontaines, Repton model of gel electrophoresis and diffusion, *J. Phys. I (France)* **1**:1759–1784 (1991).
27. J. M. J. van Leeuwen, and A. Kooiman, The drift velocity in the Rubinstein–Duke model for electrophoresis, *Physica A* 184:79–97 (1992).